CANCER GENOMICS & PROTEOMICS 2: 333-346 (2005)

Tissue Profiling by MALDI Mass Spectrometry Distinguishes Clinical Grades of Soft Tissue Sarcomas

ROBERT L. CALDWELL[1*], GINGER E. HOLT[2] and RICHARD M. CAPRIOLI[1]

[1]Mass Spectrometry Research Center and [2]Department of Orthopaedics and Rehabilitation, Vanderbilt University School of Medicine, Nashville, TN, U.S.A.

Abstract. *Soft tissue sarcomas are rare, heterogeneous, mesenchymal tumors that have been poorly classified. The heterogeneity of these aggressive tumors has made consistent tumor grading difficult and accurately predicting the behavior of the tumor based on the histological subtype and grade has been challenging. Molecular profiling of proteins in tissues may present a new avenue for distinguishing clinical grades and overall tumor aggressiveness. Direct tissue analysis using matrix-assisted laser desorption ionization mass spectrometry is a new technology that permits rapid detection of hundreds of proteins from intact tissues. We have employed this technology to profile human soft tissue sarcomas to discover protein biomarkers that distinguish tumor grade. Profiling was accomplished on histologically-stained tissue sections, allowing highly reproducible spectra for each sarcoma grade to be obtained. Forty-two tissue specimens were analyzed in this manner. Several proteins specific for high-grade sarcomas were identified and confirmed with immunohistochemistry. Proteins present in control tissue, that are suppressed by soft tissue sarcomas, were also identified.*

Soft tissue sarcomas (STS) are devastating cancers that account for 0.63% of total cancer cases and 1.15% of cancer deaths in the United States, with a five-year survival rate of approximately 60% after diagnosis (1, 2) In 2004, approximately 8,680 new cases were diagnosed in the United States, and 3,660 deaths are predicted from STS. STS are heterogeneous, mesenchymal tumors that arise from various origins, many of which are idiopathic (3). The tumors develop mostly as asymptomatic masses originating in an extremity, but can occur anywhere in the body, such as the trunk, retroperitoneum, or the head and neck (4). The current criteria set by The American Joint Committee on Cancer stages STS on histological grade, tumor size and depth, and presence of distant metastases. The most common site of metastasis is the lung parenchyma, and survival after pulmonary metastasis is <10% at two years post diagnosis (2). Pulmonary metastasis generally occurs within two to three years after diagnosis of the primary tumor (3). Despite improvements in control of local disease, mortality remains significant for more than 50% of the patients diagnosed with high-grade STS.

Currently, over fifty histological subtypes of STS exist, the most common being malignant fibrous histiocytoma (28%), leiomyosarcoma (12%), liposarcoma (15%), synovial sarcoma (10%) and malignant peripheral nerve sheath tumors (6%) (5). The heterogeneity, both intratumoral and extratumoral, of these aggressive tumors has made diagnosis, staging and treatment difficult. Anatomic pathology has been used since 1977 to categorize STS, regardless of whether or not the morphological differences indicate a certain level of tumor invasiveness or metastatic potential (6). Indeed, these unique clinical features, associated with the large variety of STS, have given rise to many histological subtypes, making the staging and grading criteria used to predict patient outcome controversial. It has been established that STS is misclassified in up to 25% to 40% of cases (7-10). Moreover, the current staging and grading criteria are not applicable to all types of STS and have no prognostic value for several histological subtypes (11). Therefore, treatment regimens remain extremely controversial due to this overwhelming, and often inaccurate, classification scheme. For this reason, the need for more objective molecular and biochemical protein biomarkers is required to improve the accuracy of conventional anatomic and histological assessments. In this respect, it is also reasonable to presume that more generalized grades exist that are based on specific protein expression profiles. These profiles may translate into disease

Current address: Vanderbilt Orthopaedic Institute, Medical Center East, South Tower, Suite 4200, Nashville, TN 37232-8774, U.S.A.

Correspondence to: Richard M. Caprioli, Ph.D., Mass Spectrometry Research Center, Vanderbilt University School of Medicine, 465 21st Avenue S., Room 9160, Medical Research Building III, Nashville, TN 37232-8575, U.S.A. e-mail: richard.m.caprioli@vanderbilt.edu

Key Words: MALDI mass spectrometry, proteomics, tissue profiling, biomarker, soft tissue sarcoma.

biomarkers that can be incorporated into standard diagnostic and treatment strategies. To accomplish this goal, we employed matrix-assisted laser desorption ionization mass spectrometry (MALDI MS) tissue profiling technology to identify protein biomarkers that discriminate between high-grade and low-grade STS.

Tissue profiling by MALDI MS, introduced in 1999, permits the measurement of protein expression patterns in cells derived in culture or in fresh tissue samples (12). With this method, a sample is mounted on a metal target plate, matrix solution is deposited in an array of small spots and each dried matrix spot is analyzed by mass spectrometry. A UV laser is used to desorb and ionize molecules from these spots. Ionized molecules are accelerated down a flight tube of a time-of-flight mass spectrometer and the mass-to-charge (m/z) ratio of each ion is calculated. The data obtained from such an analysis consist of mass spectra in which the peaks correspond to the protonated molecular forms of desorbed peptides or proteins. MALDI MS produces singly charged protonated molecules for the most part, so the m/z value represents the molecular weight of the protein plus one proton. For direct tissue analysis, multiple matrix spots can be deposited on the tissue surface and the data collected as a series of mass spectra. Each spectrum contains signals from many hundreds of proteins and peptides specific to that tissue region.

Since its introduction, MALDI MS has become an effective tool for discovering protein biomarkers from various types of cancer, including brain, lung and several other organs. For example, in a study of cancerous tissue from human prostate, MALDI MS analysis revealed over-expression of a protein PCa-24 in the cancerous tissue, indicating its potential role as a biomarker (13). Similar studies have been carried out in azoxymethane-induced colon tumors in mice (14) and biopsies obtained from patients with non-small cell lung carcinoma (15). Several tumor-specific protein biomarkers were identified in these studies. In the latter example, protein profiling allowed classification of lung cancer histologies, predicted survival, and distinguished primary tumors from metastatic tumors of the lung.

In the present work, to better characterize protein profiles acquired from potentially diverse tumor types, we employed a method that allows histological staining and MALDI MS analysis to be performed on the same tissue section for microscopic evaluation prior to MALDI MS analysis (16). Sectioned tissues are transferred to a conductive glass slide and stained with cresyl violet, a histological dye compatible with MALDI MS. Regions within the tissue section that contain compartments of cellular proliferation are identified under a light microscope and matrix is deposited on these specific regions. Using this technique, a high level of signal homogeneity between spectra from morphologically heterogeneous tissues can be obtained. For STS studies, MALDI MS tissue profiling facilitated the discovery of protein biomarkers that differentiated high-grade from low-grade STS. Additionally, extracellular matrix proteins were identified that are absent in the sarcoma tissue. Immunohistochemical staining for several of these protein species verified the MALDI MS tissue profiling data. This group of biomarkers may be useful in standardizing diagnostic and prognostic criteria for STS, and facilitate our understanding of the pathomechanisms giving rise to the disease.

Materials and Methods

IRB approval. IRB approval was obtained for procuring STS and control tissues from adult patients undergoing STS resections at Vanderbilt University Medical Center (VUMC, TN, USA). Tissues were also procured from the Cooperative Human Tissues Network at VUMC. Mass spectra from high-grade STS (30 patients, 100 spectra), low-grade STS (10 patients, 41 spectra) and skeletal muscle control (6 patients, 21 spectra) were acquired throughout the course of these studies. Each tumor grade, determined by a surgical pathologist prior to analysis, is representative of fibrosarcoma, leiomyosarcoma, liposarcoma, malignant fibrous histiocytoma, neurosarcomas and synovial sarcoma.

Tissue sectioning and staining. After surgical excision, the tissue specimens were divided for routine clinical pathology and research use. Tissue sections were snap-frozen in liquid N_2 and maintained at –80˚C until further use. Thin tissue sections (10-12 μm thick) were cut with a Leica Jung cryostat (Leica Microsystems AG, Welzlar, Germany) at –15˚C. The glass MALDI target plates were maintained at –15˚C within the cryostat chamber. The frozen sections were transferred to the cold target plates and thaw-mounted by simply warming the plate. Prior to staining, sections were dried in a desiccator for at least 30 minutes. Several hundred microliters of cresyl violet dye were directly deposited on the sections using a Pasteur pipette and allowed to react for 30 seconds. Excess stain was removed by immersing the plates for 15 seconds in two successive Petri dishes, containing 70% and 100% ethanol, respectively. The sections were allowed to dry in a desiccator for about 30 minutes. Photomicrographs of the sections were obtained under magnification using an Olympus BX 50 microscope (Olympus America Inc., Melville, NY, USA) equipped with a digital camera. Regions of cellular proliferation were identified for depositing matrix.

Sample preparation. Matrix (sinapinic acid at 30 mg/mL in a mixture of 50:50:0.1 acetonitrile/H_2O/trifluoroacetic acid by volume) was deposited in discrete droplets on the various tissue sections. For droplet deposition, two 200 nL drops of matrix were deposited onto specific regions of the tissue section after cresyl violet staining (*i.e.* regions of cellular proliferation). The first droplet was allowed to dry before the second droplet was deposited. The section was then dried in a desiccator for about 30 minutes.

MALDI MS analyses. Mass spectrometric analyses were performed in the positive linear mode at +25 kV of accelerating potential on an Applied Biosystems Inc. (Framingham, MA, USA) Voyager DE-STR time-of-flight mass spectrometer. The instrument is equipped with a 337 nm N_2 laser operating at a 20 Hz repetition

rate. One thousand laser shots were acquired per spot with 2-4 matrix spots per tissue section. Each mass spectrum was externally calibrated from a protein mixture containing porcine insulin (*m/z* 5,777.60), bovine cytochrome c (*m/z* 12,232.0), equine apomyoglobin (*m/z* 16,952.0), and bovine trypsinogen (*m/z* 23,976.0), and internally calibrated with peaks from hemoglobin alpha (*m/z* 15,126.3) and beta (*m/z* 15,867.2) chains. Mass spectra were processed using Data Explorer software (Applied Biosystems).

Protein identification

Sample preparation and digestion: Approximately 300 mg of tissue were suspended in homogenization buffer, homogenized and further prepared for HPLC separation as described in (17). After separation, fractions containing the proteins of interest were further separated using 1-dimensional SDS on a 4-12% Bis Tris precast gel (Invitrogen, Carlsbad, CA, USA) for 35 minutes at 200 V. All gels were fixed with 50% methanol, 10% acetic acid for 15 minutes and then stained with Colloidal Blue overnight, followed by destaining with water. Discrete bands representing the molecular weights of the *m/z* signals observed in the MALDI spectra were excised from the gel and equilibrated in ammonium bicarbonate buffer (0.4 mol/L, 25 μL) and reduced with DTT (5 μL, 45 mmol/L) for 15 minutes at 60˚C and alkylated with iodoacetimide (5 μL, 100 mmol/L) for 15 minutes at room temperature in the dark. Trypsin (0.05 μg) was added and the samples were digested for 24 hours at 37˚C. Peptides were extracted using 60% acetonitrile/ 40% 0.1% TFA (3 x 100 mL), pooled and dried. Samples were reconstituted in 0.1% TFA and desalted using a C18 ZipTiP (Millipore, Bedford, MA, USA), according to the manufacturer's protocol, and kept at 4˚C until further analysis.

LC-MS/MS analysis: LC-MS/MS analyses were performed on a ThermoFinnigan LTQ linear ion trap mass spectrometer equipped with a ThermoFinnigan Surveyor quanterery HPLC pump and a microelectrospray source (Thermo Electron, San Jose, CA, USA). Reversed-phased separation of the tryptic peptides was performed using fused silica capillary tips (Polymicro Technologies, Phoeniz, AZ, USA; 100 μm i.d., 360 μm o.d.) packed with Monitor C18 (5 μm, Column Engineering, Ontario, CA, USA). The HPLC pump was operated at a flow rate of 175 μL/min and was split to achieve a flow through the column of 700 nL – 1000 nL min^{-1}. Mobile phase A consisted of 0.1% formic acid and mobile phase B consisted of 0.1% formic acid in acetonitrile. After equilibrating the column with 100% A, the peptides were eluted off the column with a gradient of 5% B for 5 minutes, increased to 50% B by 50 minutes, then increased to 80% by 52 minutes, increased to 90% by 55 minutes and held for 1 minutes. The gradient was then returned to 5% B over the next 5 minutes and continued at that composition until the end of the run at 71 minutes. LTQ ion trap mass spectrometer and HPLC solvent gradients were controlled by Xcalibur 1.4 software (Thermo Electron).

MS/MS spectra were acquired using a data-dependent scanning mode with one full MS scan (400-2000 m/z) followed by three MS/MS scans of the three most intense precursor masses at 35% collision energy. Tandem mass spectra from LC-MS/MS analyses were searched against the human database using SEQUEST (Thermo Electron) and the data filtered using a custom-designed software tool (Complete Heirarchical Integration of Protein Searches, CHIPS) (18) based upon the following filtering criteria: cross correlation (Xcorr) value of >1.8 for doubly-charged ions, and >2.5 for triply-charged ions. An RSp (ranking of primary score) value of <5 and a Sp value (primary score) >350 were also required for positive peptide identifications that match to the intact protein. Parallel controls were performed during each step of the protein identification process (HPLC separation, gel electrophoresis, LC-MS) using protein standards to verify the efficacy and reproducibility of the analysis.

Immunohistochemistry

Calcyclin: Tissue sections from control tissue, low- and high-grade STS were paraffin embedded and sectioned (5 μm) in a microtome. The sections were floated over a warm water bath (40˚C) and transferred to a slide and baked overnight. The slides were depariffinized through 2 changes of xylene for 20 minutes each, then 2 changes each of 100% and 95% alcohol for 10 minutes each. The slides were placed in a PBS buffer solution, then incubated in 95˚C target retrieval solution (TRS, citrate buffer) for 20 minutes and allowed to cool for 20 minutes in TRS. The slides were transferred back into PBS buffer. Peroxidase blocking reagent (100 μL) was placed on each section and allowed to stand for 10 minutes. After a buffer rinse, 100 μL of protein block was added to each section for 10 minutes followed by another buffer rinse. A 1:1000 dilution of S-100A6 (Sigma, St. Louis, MO, USA) was then added in 100 μL portions to each section and left to incubate overnight at 4˚C and the slides were rinsed with buffer the following day. The secondary antibody, a labeled mouse/rabbit dual polymer with peroxidase, was added for 30 minutes (100 μL/section). Another buffer rinse was followed by a 3-minute distilled water step, with 100 μL of DI H_2O added to each section. Two more buffer rinses were followed by addition of DAB + (100 μL/section) for a 10-minute incubation period. The slides were briefly rinsed in buffer and counterstained with hematoxylin for approximately 1 minute, followed by a 5-minute water rinse to remove any excess hematoylin. The slides were cleared of water through 2 changes each of 95% and 100% alcohol for 10 dips. Following 1 minute sessions through 2 changes of xylene, the slides were permanently secured with mounting media and cover glass.

Calgranulin: Five-micron sections of paraffin-embedded tissues were placed on charged slides and the paraffin was removed. The sections were rehydrated and placed in heated Target Retrieval Solution (DakoCytomation, Carpinteria, CA, USA) for 20 minutes. Endogenous peroxidase was neutralized with 0.03% hydrogen peroxide and the samples were treated with diluted rabbit serum prior to primary antibody addition. The tissues were incubated with goat anti-Calgranulin (Santa Cruz Biotechnology, Santa Cruz, CA, USA) diluted 1:500 for 30 minutes. Sections without primary antibody served as negative controls. The Vectastain ABC Elite (Vector Laboratories, Inc., Burlingame, CA, USA) System and DAB+ (DakoCytomation) was used to produce localized, visible staining. Slides were lightly counterstained with Mayer's hematoxylin, dehydrated and coverslipped.

Macrophage migration inhibitory factor (MIF): Five-micron sections were placed on charged slides. Endogenous peroxidase activity was inactivated with 0.03% hydrogen peroxide. The sections were incubated with rabbit polyclonal anti-MIF (Santa Cruz Biotechnology) diluted 1:50 for 60 minutes. Sections without primary antibody served as negative controls. The Dako Envision+ System, DAB/Peroxidase (DakoCytomation) was used to produce localized, visible staining. The slides were lightly counterstained with Mayer's hematoxylin, dehydrated and coverslipped.

Myosin light chain 2 (MLC-2): Five-micron sections of frozen tumor tissues were placed on charged slides. The slides were acetone-fixed and gently rinsed. To minimize nonspecific protein binding, 1.5% rabbit serum was applied to the slides for 20 minutes. The sections were treated overnight with goat anti-MLC2 (Santa Cruz Biotechnology) diluted 1:50 at 2˚C. Endogenous peroxidase was neutralized with 0.03% hydrogen peroxide. Sections without primary antibody served as negative controls. The Vectastain ABC Elite (Vector Laboratories, Inc) System and DAB+ (DakoCytomation) was used to produce localized, visible staining. Slides were lightly counterstained with Mayer's hematoxylin, dehydrated and coverslipped.

Vimentin: Five-micron sections were placed on charged slides and the paraffin was removed. The sections were rehydrated and placed in heated Target Retrieval Solution (DakoCytomation) for 20 minutes. Endogenous peroxidase activity was inactivated with 0.03% hydrogen peroxide followed by a casein solution (DakoCytomation) for blocking interfering protein interactions. The sections were incubated with mouse anti-vimentin (DakoCytomation) diluted 1:100 for 20 minutes. Sections without primary antibody served as negative controls. The Dako Envision+ System, mouse/HRP (DakoCytomation) was applied for 30 minutes. Visible results were produced with DAB and the tissues were counterstained with Mayer's hematoxylin prior to coverslipping.

Statistical analyses. All mass spectra were converted to text files and imported into ProTSData Version 1.1 (Effekta, Steamboat Springs, CO, USA) for baseline correction and normalization by total ion current (TIC) in batch mode. A standard weighted-means-averaging (WMA) algorithm was then applied. The weight value (W) is a statistically derived function that approaches significance as the distance between the means (μ) for each group increases and the SD (σ) decreases using the formula, $W = (\mu^1-\mu^2)/(\sigma^1+\sigma^2)$. Thus, the most significant protein peaks were then used as the top weighted data-points (*m/z* intensities) (19, 20). In this way, *m/z* values were filtered according to the highest weight which best differentiated the normal *versus* cancer groups. Further filtering was carried out (1) to exclude values with WMAs less than 1.0 (similar in respect to 2 σ from the mean control value), and (2) to exclude mean intensity differences that fell below two fold (cut-off value for tissue profiling, data not published). The filtered values were then used for peak detection, and further evaluated by plotting the entire spectrum in Origin 7.0. The Tukey method was used for multiple comparisons to determine the statistical significance between low-grade, high-grade STS and control tissues by comparing peak heights (apex) of each specific *m/z*. Bar graphs and confidence ranges (±SD) were prepared by entering peak heights of each statistically different *m/z* into the software package InStat (GraphPad Software, San Diego, CA, USA).

Results

MALDI MS protein profiles from high-grade STS, low-grade STS and control tissues were acquired, calibrated, baseline corrected and normalized. Care was taken to maintain the same instrument settings, cresyl violet staining conditions and data processing parameters throughout the study. Averaged spectra representing each condition (high-grade, low-grade, control) were overlaid and compared to identify protein species that may discriminate between tumor grades and healthy control tissues. Figures 1A and 1B show mass spectra from *m/z* 10,000-16,000 and *m/z* 16,000–22,000, respectively. These data show relative abundances of several proteins comparing (1) high-grade to low-grade STS, and (2) STS to control tissues. Many signals are differentially expressed between high-grade, low-grade and control tissues, including *m/z* 11,651, 10,092, 12,338, 10,835, 14,007, 15,333, 13,775 and 11,305. These proteins have been identified in other cancers and represent potential biomarkers that may be useful to distinguish high-grade from low-grade tumors.

Proteins that appear differentially expressed in Figure 1 were tested for statistical significance using ANOVA, as described in the Methods section. Statistically significant *m/z* differentiating high-grade STS from low-grade STS and control tissues are shown in Figure 2. These include *m/z* (±S.D.) consistent with proteins previously identified in other tissues, including calgizzarin (21), calcyclin (21), macrophage inhibitory factor (22) and calgranulin (23). Several proteins were also observed that were consistently absent in the cancerous tissue compared to control tissues, including *m/z* 18,945 (myosin light chain-1), 21,069 (myosin light chain-2), and 21,854 (myosin light polypeptide 3). Additionally, *m/z* 53,660 (vimentin) was found to be up-regulated in both high- and low-grade STS compared to control tissue. These proteins were identified as described in the Methods section. Except for histone H3, relatively high mass accuracy was observed among each *m/z* of interest. The S.D. observed for histone H3 (± 10 Da) is mostly the result of the net effect of multiple post-translational modifications. In keeping with traditional microscopic observations, histone expression was increased in the high-grade STS compared to the low-grade STS and control tissues. These *m/z* are consistent with histones previously identified in other tissues (H2A.2 (diacetylated) (24), H3 (modified) (25), H4 (dimethylated, monoacetylated) (25) and H2BA (native, http://ca.expasy.org/uniprot/P62807). The assignment of *m/z* 13,775 detected in the tissue profiling experiments to histone H2BA in the Swiss-Prot database is theoretical and requires further analysis as described in the Methods section to verify its identification.

To identify proteins whose levels were suppressed in cancerous tissues, tissue homogenates were first semi-purified by high performance liquid chromatography followed by one-dimensional SDS-PAGE. Discrete gel bands, whose migrations were consistent with the *m/z* value of the masses of interest, were subjected to in-gel digestion followed by LC-MS/MS analysis. Each protein was matched by multiple peptide identifications that corresponded in mass to discriminatory peaks. An example of peptides matching to the intact protein and score values are shown in Table I.

While altered histone expression is common among different cancer grades, other proteins differentially expressed in the

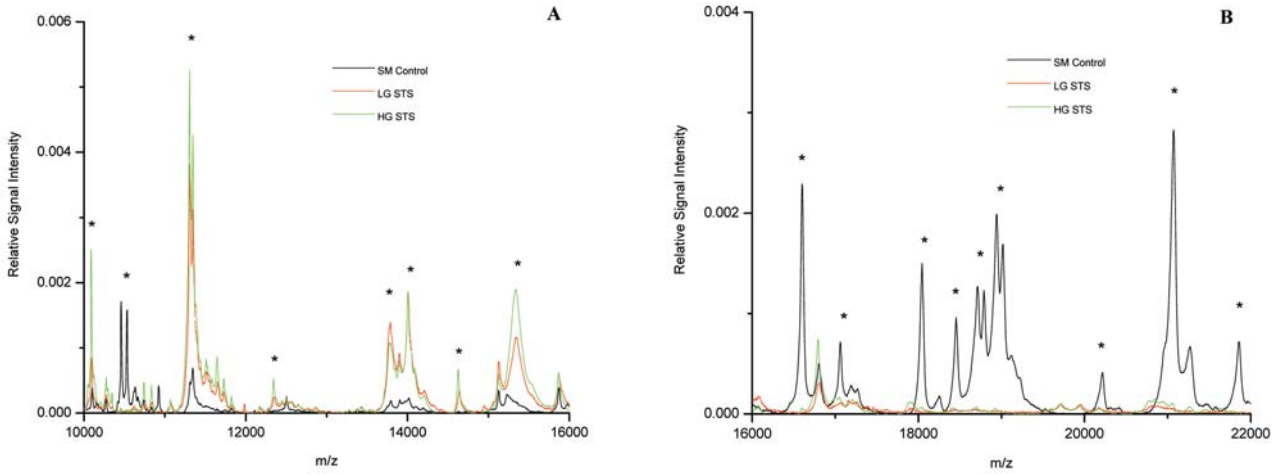

Figure 1. *Averaged mass spectra from high-grade STS, low-grade STS, and skeletal muscle control from m/z 10,000-16,000 (Figure 1A) and m/z 16,000-22,000 (Figure 1B). Protein profiles from each category were externally and internally calibrated, baseline corrected and normalized before averaging and overlaying, as detailed in the Methods section. Signals with differential expression between tumors and normal tissue upon visual analysis are highlighted by asterisks.*

tissue profiling experiments were validated by immunohistochemistry when appropriate antibodies were available. Immunostaining for calcyclin (*m/z* 10,090), MIF (*m/z* 12,338), calgranulin (*m/z* 10,835), MLC-2 (*m/z* 21,069) and vimentin (*m/z* 53,660) was accomplished on high- and low-grade STS, and control tissue sections to corroborate observations made from MALDI MS tissue profiling (Figure 3). In agreement with the tissue profiling spectra and previous studies, a significant increase in calcyclin, MIF and calgranulin expression was observed from the high-grade STS relative to the low-grade and control tissues. As expected, an increase in vimentin staining was observed in both STS grades compared to control tissue, and the expression of MLC-2 was very low in both sarcoma grades compared to that of the control.

Table I. *An example of tandem mass spectra from LC-MS-MS analysis used to search against a non-redundant human database using data filtered using CHIPS, as described in the Methods section. An RSp value of < 5 and a Sp value > 350 were also required for positive peptide identifications that match to the intact protein (data not shown).*

Protein	Intact MW (Da)	Coverage	Peptides Sequenced
Vimentin	53662.9	36.2%	FANYIDK
			LGDLYEEEMR
			RQVDQLTNDK
			EKLQEEMLQR
			LQEEMLQR
			QDVDNASLAR
			NLQEAEEWYK
			FADLSEAANR
			QVQSLTCEVDALK
			LQDEIQNMK
			LLEGEESR
			ETNLDSLPLVDTHSK

Discussion

Histological staining of high-grade STS, low-grade STS and control tissue prior to MALDI MS analysis permitted the acquisition of highly homologous spectra from each tissue specimen. Data analyses revealed many differences in protein expression patterns that allowed discrimination between high-grade and low-grade STS. These data also showed that several proteins are consistently absent in STS tissue compared to the healthy tissues. Immunohistochemical staining of tissues verified several of the results from the MALDI MS profiling experiments.

A limitation in this study, intrinsic to sarcoma research, is the low number of STS samples available for study. STS is a rare form of cancer that accounts for 0.63% of the total cancer cases in the United States and so the number of human biopsies is small. Several proteins we found to be specific for high-grade STS have also been identified in other highly invasive cancers. A recent study by Cmogorac-Jurcevic *et al.* reported a high prevalence of calcyclin dysregulation in pancreatic carcinoma (26). Another study has reported overexpression of calcyclin in invasive margins of colorectal carcinomas (27). Although the specific function of calcyclin is not completely understood,

Figure 2.

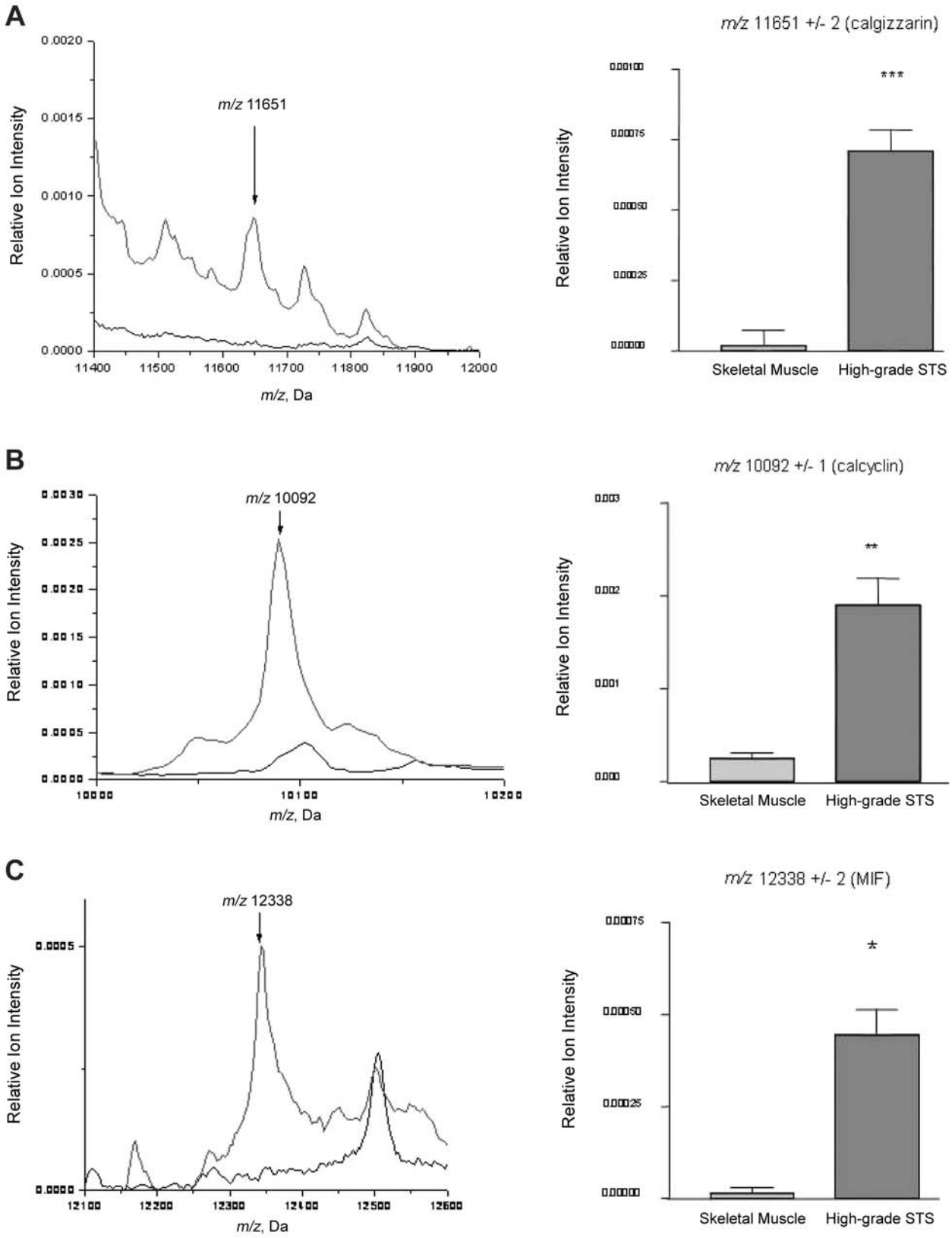
A
m/z 11651
Relative Ion Intensity
m/z, Da
m/z 11651 +/- 2 (calgizzarin)
***
Skeletal Muscle
High-grade STS
B
m/z 10092
Relative Ion Intensity
m/z, Da
m/z 10092 +/- 1 (calcyclin)
**
Skeletal Muscle
High-grade STS
C
m/z 12338
Relative Ion Intensity
m/z, Da
m/z 12338 +/- 2 (MIF)
*
Skeletal Muscle
High-grade STS

Figure 2. *continued*

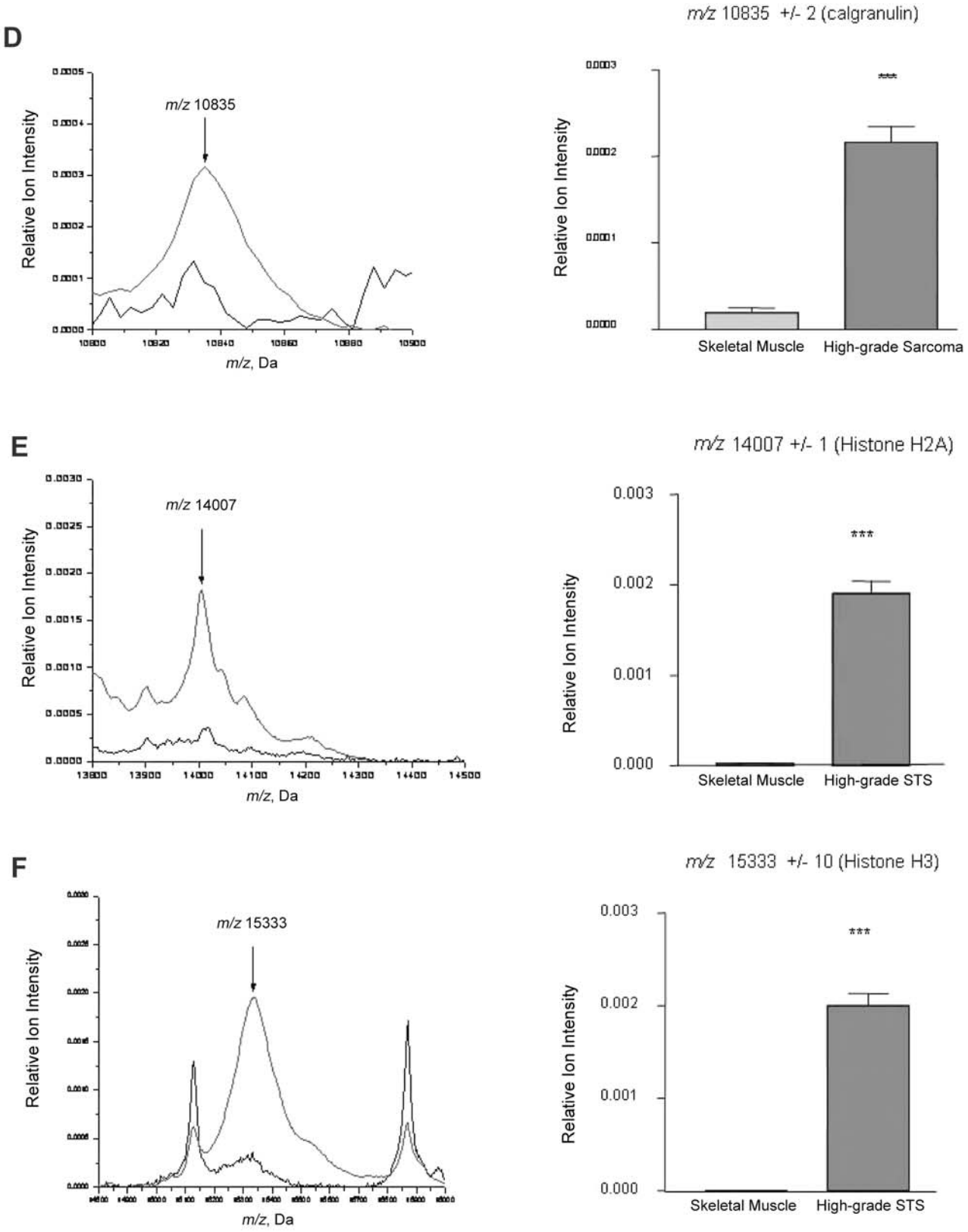

Figure 2. *continued*

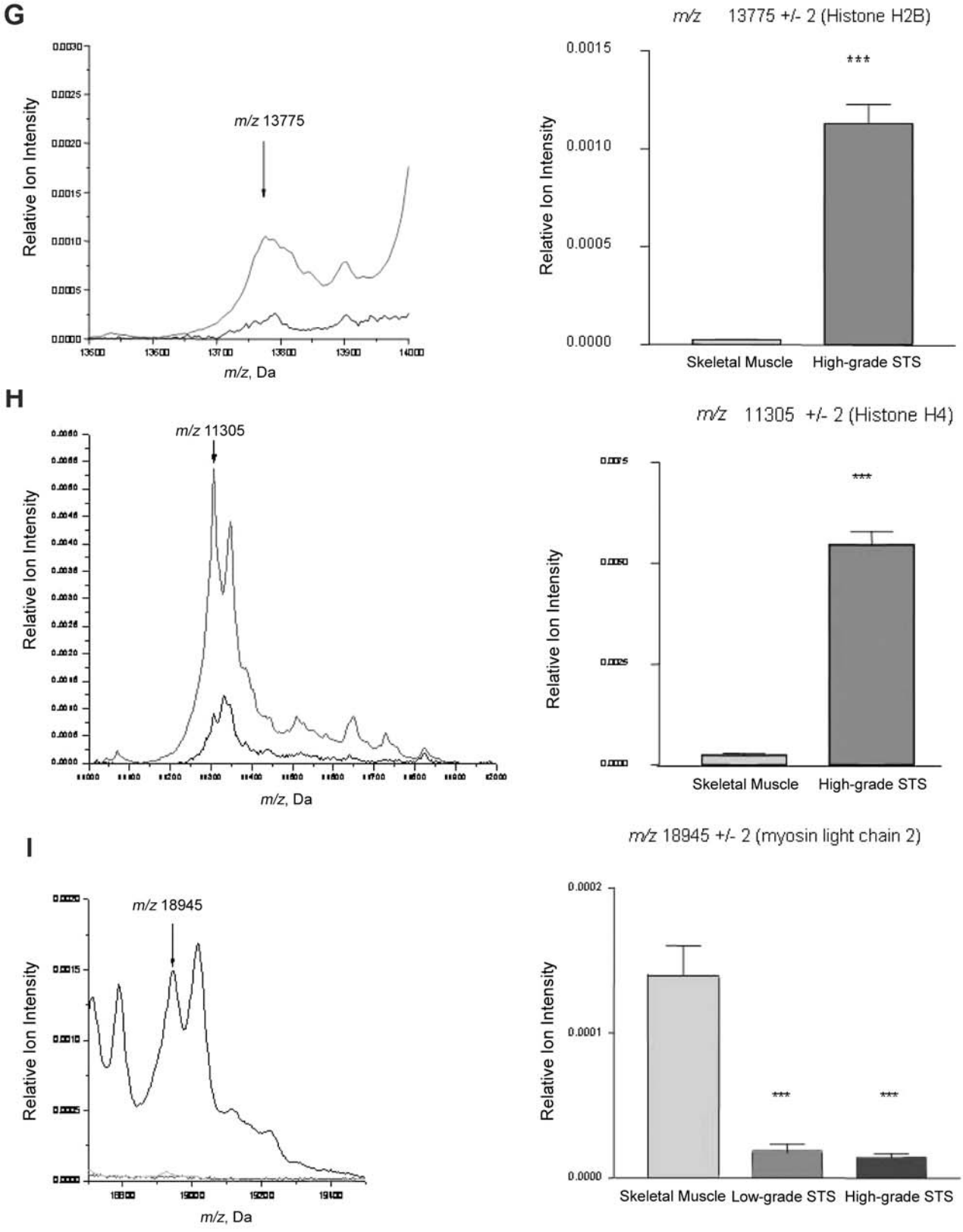

Figure 2. *continued*

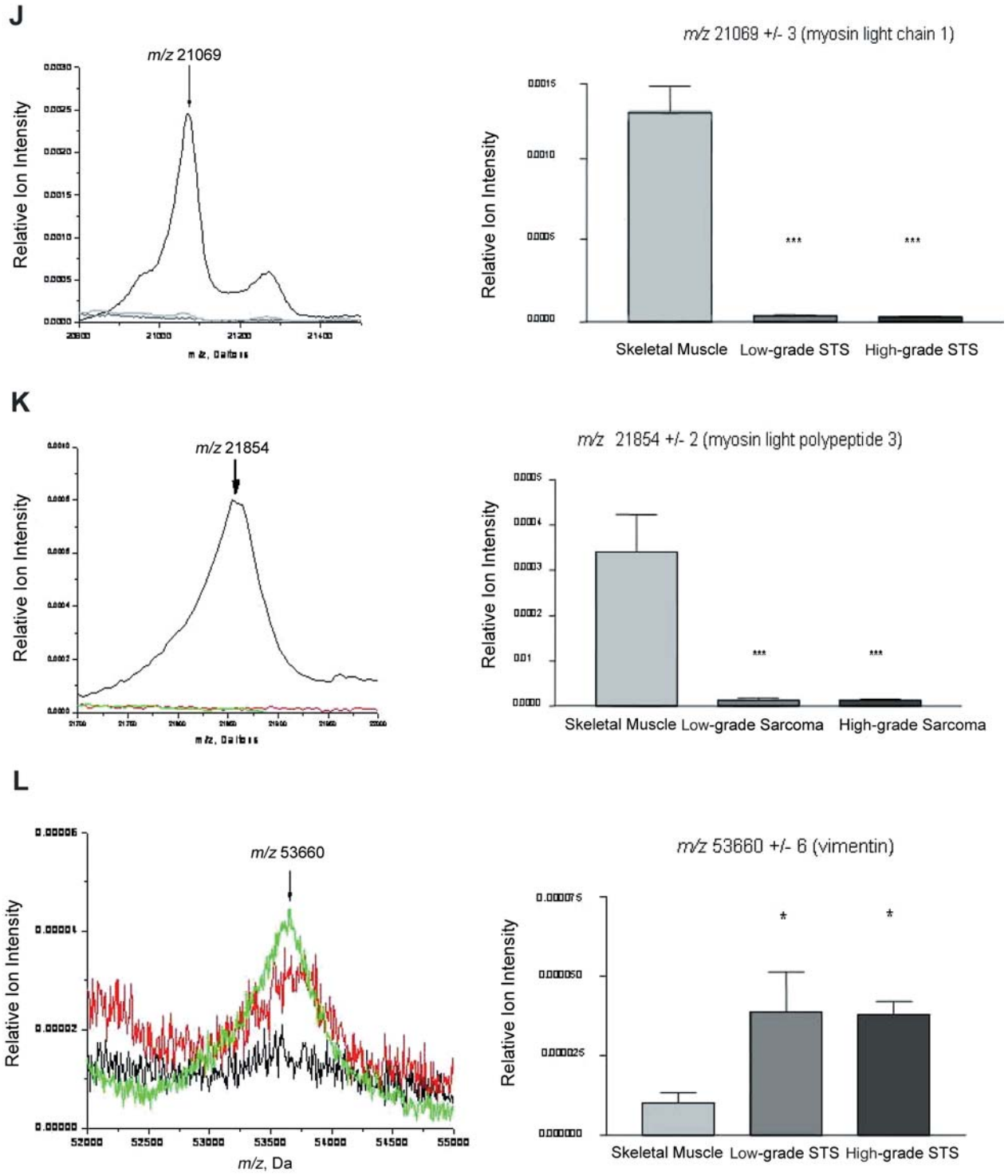

Figure 2. *Selected mass spectral regions showing the m/z (±S.D.) of differentially-expressed proteins between control tissues, low-grade and high-grade STS prior to statistical analysis. For figure panels 2A-2H, red lines represent high-grade STS and black-lines represent control tissues. No statistical differences were observed between low-grade STS and control tissue for the given peaks in panels 2A-2H. For figure panels 2I-2L, black lines represent control tissues, red lines represent low-grade STS and green lines represent high-grade STS. Peaks that were statistically different were identified as described in the Methods section. After normalization, peak heights were used to compute statistical significance *=p<0.05, **=p<0.01, ***=p<0.001 comparing control to high-grade STS (panels 2A-2H) and comparing both sarcoma grades to control tissue (panel 2I-2L).*

it is a member of the S100 family of genes that share a similar structure and function in the cell. Generally, these are small (9-12 kD), structurally homologous calcium-binding proteins that have multiple cellular functions (28), including phosphorylation inhibition of annexin, myosin heavy chain and p53. The S100 family members also interact with cytoskeletal elements, including microtubules and actin, leading to dysfunction in microtubule assembly and increased motility and invasion (29). Our studies also identified overexpression of calgranulin in high-grade STS, a protein also shown to exist in cystic fluid and sera from patients diagnosed with ovarian cancer (30). Additionally, increased levels of calgranulin were found in the urine and prostatic cancer tissue (31). These studies suggest a putative role for calgranulin as a biomarker for several cancer types from a variety of biological sources. Macrophage migration inhibitory factor (MIF) has been recently implicated in regulating tumor migration and expression of angiogenic factors in hepatocellular carcinoma (32), as well as in the regulation of host inflammatory and immune responses. Under normal physiological conditions, MIF circulates at basal levels in the serum, and additional MIF is secreted as an immune response from activated monocytes and macrophages (33-35). In addition, MIF has been linked to fundamental processes that control cell proliferation, differentiation, angiogenesis and tumor progression (36). In one recent report, MIF was shown to inactivate the tumor suppressing activity of p53 (37), while overexpression of MIF has recently been observed in human melanoma (38), breast carcinoma (39), metastatic prostate cancer (40) and adenocarcinoma of the lung (41). MIF levels were significantly higher in the sera from patients with hepatocellular carcinoma compared to that from controls.

Our studies have also shown that myosin light chain (MLC)-1 and -2, and myosin light polypeptide-3, abundantly expressed in control tissues, were not detectable in our analyses in both low- and high-grade STS. Two recent reports showed altered expression of myosin in cancer cachexia (42), and that these events are a selective, specific process (43). Given that STS invades a variety of tissues, including bone, skeletal muscle, fat and cartilage, remodeling of the extracellular matrix is most probably a key event for hyperplasia and metastasis. Further studies, that examine the specificity and identify the molecules involved in the STS-mediated degradation of the extracellular matrix, may shed light into STS invasion and reveal therapeutic targets that may be used to inhibit tumor growth.

Vimentin was found to be overexpressed in both sarcoma grades compared to control tissues, consistent with its current role as a clinical marker for sarcomas (44-47). A member of the type III family of intermediate filaments, vimentin, plays a key role in the dynamic remodeling of the cell during development of the neoplastic phenotype (48), and has recently been reported to serve as a protein marker to predict resistance to topoisomerase inhibitors (*i.e.* etoposide) in neuroblastoma (49). Vimentin is one of the substrates cleaved by caspases and is part of the execution phase of apoptosis (50). The significant increase of vimentin expression may represent a molecular mechanism to renew the caspase-cleaved vimentin in order to maintain cell integrity and counteract apoptosis.

Results from present and future studies stemming from this research will have significant scientific and clinical implications. Clinically, protein markers for sarcomas can be used to more accurately correlate individual tumor biology and patient outcome and more accurately define tumor grades. This would greatly assist the clinician in designing a more appropriate patient treatment strategy based upon established protein biomarkers. Overexpression of specific proteins in high-grade STS, such as calcyclin, may lead to the release of this protein into the patient's bloodstream or urine. Detection of these biomarkers in the serum and/or urine could serve as reliable markers to differentiate tumor grade, or to aid in tumor surveillance after treatment. Non-specific blood tests already exist that are suggestive of several orthopaedic disorders, such as expression of alkaline phosphatase for Paget's Disease (51). Moreover, the relatively large tissue masses that make up STS (often several centimeters in diameter) increase the likelihood of passive protein diffusion into the circulation as compared to other tumor types.

Because the predicted survival of STS patients after pulmonary metastasis is poor (<10% survival at two years), the ability to ascertain whether the primary tumor has pulmonary metastatic potential would be highly significant. Further studies, using MALDI MS tissue profiling to compare protein expression patterns between the primary tumor and pulmonary metastatic tumor, might reveal such protein markers. This work may also have important therapeutic value since STS may range from histological subtypes that are very responsive to cytotoxic chemotherapy to subtypes that are quite resistant to current agents. A major deterrent to the use of adjuvant chemotherapy has been the risk of causing adverse toxic effects in patients who do not otherwise respond to therapy. By identifying biomarkers associated with high-grade and pulmonary

→

Figure 3. *Immunohistochemical staining (40X magnification) for high-grade STS biomarkers and MLC-2 from (A) skeletal muscle control, (B) low-grade STS (C) and high-grade STS. Note that the abundance of immunostaining staining observed from the high-grade STS section compared to control tissue is comparable to the MALDI MS profiling data.*

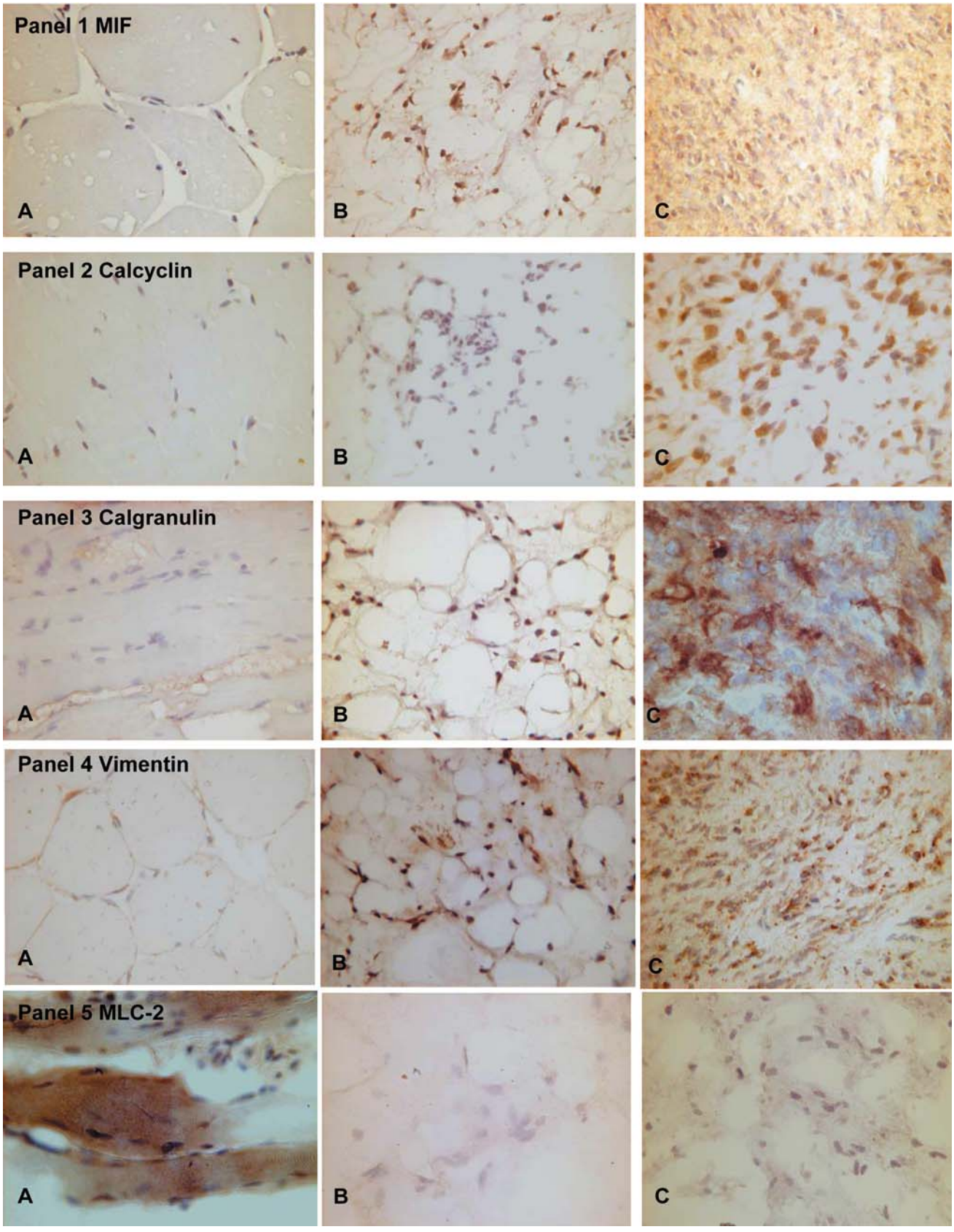
Panel 1 MIF
A
B
C
Panel 2 Calcyclin
A
B
C
Panel 3 Calgranulin
A
B
C
Panel 4 Vimentin
A
B
C
Panel 5 MLC-2
A
B
C

metastatic STS, therapeutic interventions specifically directed to STS might be considered.

Acknowledgements

The authors acknowledge funding support from NIH/NCI/NIDA 5R33 CA86243 and NIH/NIGMS 5R01 GM58008 (RMC). The expert assistance of Lillian B. Nanney, Ph.D., and Kelly S. Parman (VUMC Mouse Pathology and Immunohistochemistry Core Laboratory) are acknowledged. The authors also acknowledge Herbert S. Schwartz, MD, Tom Bradbury, MD, Lisa Zimmerman, Ph.D., Jim Mobley, Ph.D., Jeremy L. Norris, Ph.D., and Deming Mi, MS, for help in acquiring these data.

References

1 Jemal A, Tiwari RC, Murray T, Ghafoor A, Samuels A, Ward E, Feuer EJ and Thun MJ: Cancer statistics. CA Cancer J Clin *54*: 8-29, 2004.

2 Pisters P: American Cancer Society Atlas of Clinical Oncology: Soft Tissue Sarcomas. Edited by Pollock RE. Hamilton, Ontario, BC Decker, pp. 80-88 , 2002.

3 Cormier JN and Pollock RE: Soft tissue sarcomas. CA Cancer J Clin *54*: 94-109, 2004.

4 DeVita VT Jr and Rosenberg SA: Cancer: Principles and Practice of Oncology. Edited by Philadelphia, Lippincott Williams & Wilkins, pp. 1841-1891, 2001.

5 Coindre JM, Terrier P, Guillou L, Le Doussal V, Collin F, Ranchere D, Sastre X, Vilain MO, Bonichon F and N' Guyen Bui B: Predictive value of grade for metastasis development in the main histologic types of adult soft tissue sarcomas: a study of 1240 patients from the French Federation of Cancer Centers Sarcoma Group. Cancer *91*: 1914-1926, 2001.

6 Russell WO, Cohen J, Enzinger F, Hajdu SI, Heise H, Martin RG, Meissner W, Miller WT, Schmitz RL and Suit HD: A clinical and pathological staging system for soft tissue sarcomas. Cancer *40*: 1562-1570, 1977.

7 Singer S: New diagnostic modalities in soft tissue sarcoma. Sem Surg Oncol *17*: 11-22, 1999.

8 Shiraki M, Enterline HT, Brooks JJ, Cooper NS, Hirschl S, Roth JA, Rao UN, Enzinger FM, Amato DA and Borden EC: Pathologic analysis of advanced adult soft tissue sarcomas, bone sarcomas, and mesotheliomas. The Eastern Cooperative Oncology Group (ECOG) experience. Cancer *64*: 484-490, 1989.

9 Presant CA, Russell WO, Alexander RW and Fu YS: Soft-tissue and bone sarcoma histopathology peer review: the frequency of disagreement in diagnosis and the need for second pathology opinions. The Southeastern Cancer Study Group experience. J Clin Oncol *4*: 1658-1661, 1986.

10 Alvegard TA and Berg NO: Histopathology peer review of high-grade soft tissue sarcoma: the Scandinavian Sarcoma Group experience. J Clin Oncol *7*: 1845-1851, 1989.

11 Fletcher DM, Unni KK and Mertens F: World Health Organization Classification of Tumors: Pathology and genetics of tumours of soft tissue and bone. Edited by Washington, D.C., IARC Press, 2002.

12 Chaurand P, Stoeckli M and Caprioli RM: Direct profiling of proteins in biological tissue sections by MALDI mass spectrometry. Anal Chem *71*: 5263-5270, 1999.

13 Zheng Y, Xu Y, Ye B, Lei J, Weinstein MH, O'Leary MP, Richie JP, Mok SC and Liu BC: Prostate carcinoma tissue proteomics for biomarker discovery. Cancer *98*: 2576-2582, 2003.

14 Chaurand P, DaGue BB, Pearsall RS, Threadgill DW and Caprioli RM: Profiling proteins from azoxymethane-induced colon tumors at the molecular level by matrix-assisted laser desorption/ionization mass spectrometry. Proteomics *1*: 1320-1326, 2001.

15 Yanagisawa K, Shyr Y, Xu BJ, Massion PP, Larsen PH, White BC, Roberts JR, Edgerton M, Gonzalez A, Nadaf S, Moore JH, Caprioli RM and Carbone DP: Proteomic patterns of tumour subsets in non-small-cell lung cancer. Lancet *362*: 433-439, 2003.

16 Chaurand P, Schwartz SA, Billheimer D, Xu BJ, Crecelius A and Caprioli RM: Integrating histology and imaging mass spectrometry. Anal Chem *76*: 1145-1155, 2004.

17 Reyzer ML, Caldwell RL, Dugger TC, Forbes JT, Ritter CA, Guix M, Arteaga CL and Caprioli RM: Early changes in protein expression detected by mass spectrometry predict tumor response to molecular therapeutics. Cancer Res *64*: 9093-9100, 2004.

18 Ham AJ, Jones JA and Liebler DC: CHIPS (Complete Hierarchical Integration of Protein Searches), a database program for storing, filtering and comparing Sequest outputs. Edited by Nashville, TN, USA, 2004.

19 Golub TR, Slonim DK, Tamayo P, Huard C, Gaasenbeek M, Mesirov JP, Coller H, Loh ML, Downing JR, Caligiuri MA, Bloomfield CD and Lander ES: Molecular classification of cancer: class discovery and class prediction by gene expression monitoring. Science *286*: 531-537, 1999.

20 Kachigan SK: Multivariate Statistical Analysis: A Conceptual Introduction. Edited by Marylan: Radius Press, 1991.

21 Schwartz SA: Proteomic-based Classification of Human Brain Tumors by Mass Spectrometry. Edited by Nashville, Vanderbilt University, pp. 139, 2004.

22 Campa MJ, Wang MZ, Howard B, Fitzgerald MC and Patz EF Jr: Protein expression profiling identifies macrophage migration inhibitory factor and cyclophilin a as potential molecular targets in non-small cell lung cancer. Cancer Res *63*: 1652-1656, 2003.

23 Chaurand P, Sanders ME, Jensen RA and Caprioli RM: Proteomics in diagnostic pathology: profiling and imaging proteins directly in tissue sections. Am J Pathol *165*: 1057-1068, 2004.

24 Masumori N, Thomas TZ, Chaurand P, Case T, Paul M, Kasper S, Caprioli RM, Tsukamoto T, Shappell SB and Matusik RJ: A probasin-large T antigen transgenic mouse line develops prostate adenocarcinoma and neuroendocrine carcinoma with metastatic potential. Cancer Res *61*: 2239-2249, 2001.

25 Reyzer ML, Hsieh Y, Ng K, Korfmacher WA and Caprioli RM: Direct analysis of drug candidates in tissue by matrix-assisted laser desorption/ionization mass spectrometry. J Mass Spectrom *38*: 1081-1092, 2003.

26 Crnogorac-Jurcevic T, Missiaglia E, Blaveri E, Gangeswaran R, Jones M, Terris B, Costello E, Neoptolemos JP and Lemoine NR: Molecular alterations in pancreatic carcinoma: expression profiling shows that dysregulated expression of S100 genes is highly prevalent. J Pathol *201*: 63-74, 2003.

27 Stulik J, Osterreicher J, Koupilova K, Knizek J, Bures J, Jandik P, Langr F, Dedic K, Schafer BW and Heizmann CW: Differential expression of the Ca^{2+} binding S100A6 protein in normal, preneoplastic and neoplastic colon mucosa. Eur J Cancer *36*: 1050-1059, 2000.

28 Schafer BW, Wicki R, Engelkamp D, Mattei MG and Heizmann CW: Isolation of a YAC clone covering a cluster of nine S100 genes on human chromosome 1q21: rationale for a new nomenclature of the S100 calcium-binding protein family. Genomics *25*: 638-643, 1995.
29 Donato R: S100: a multigenic family of calcium-modulated proteins of the EF-hand type with intracellular and extracellular functional roles. Int J Biochem Cell Biol *33*: 637-668, 2001.
30 Ott HW, Lindner H, Sarg B, Mueller-Holzner E, Abendstein B, Bergant A, Fessler S, Schwaerzler P, Zeimet A, Marth C and Illmensee K: Calgranulins in cystic fluid and serum from patients with ovarian carcinomas. Cancer Res *63*: 7507-7514, 2003.
31 Rehman I, Azzouzi AR, Catto JW, Allen S, Cross SS, Feeley K, Meuth M and Hamdy FC: Proteomic analysis of voided urine after prostatic massage from patients with prostate cancer: a pilot study. Urology *64*: 1238-1243, 2004.
32 Ren Y, Tsui HT, Poon RT, Ng IO, Li Z, Chen Y, Jiang G, Lau C, Yu WC, Bacher M and Fan ST: Macrophage migration inhibitory factor: roles in regulating tumor cell migration and expression of angiogenic factors in hepatocellular carcinoma. Int J Cancer *107*: 22-29, 2003.
33 Bernhagen J, Calandra T, Mitchell RA, Martin SB, Tracey KJ, Voelter W, Manogue KR, Cerami A and Bucala R: MIF is a pituitary-derived cytokine that potentiates lethal endotoxaemia. Nature *365*: 756-759, 1993.
34 Calandra T, Bernhagen J, Mitchell RA and Bucala R: The macrophage is an important and previously unrecognized source of macrophage migration inhibitory factor. J Exp Med *179*: 1895-1902, 1994.
35 Calandra T, Bernhagen J, Metz CN, Spiegel LA, Bacher M, Donnelly T, Cerami A and Bucala R: MIF as a glucocorticoid-induced modulator of cytokine production. Nature *377*: 68-71, 1995.
36 Mitchell RA and Bucala R: Tumor growth-promoting properties of macrophage migration inhibitory factor (MIF). Sem Cancer Biol *10*: 359-366, 2000.
37 Hudson JD, Shoaibi MA, Maestro R, Carnero A, Hannon GJ and Beach DH: A proinflammatory cytokine inhibits p53 tumor suppressor activity. J Exp Med *190*: 1375-1382, 1999.
38 Shimizu T, Abe R, Nakamura H, Ohkawara A, Suzuki M and Nishihira J: High expression of macrophage migration inhibitory factor in human melanoma cells and its role in tumor cell growth and angiogenesis. Biochem Biophys Res Commun *264*: 751-758, 1999.
39 Bini L, Magi B, Marzocchi B, Arcuri F, Tripodi S, Cintorino M, Sanchez JC, Frutiger S, Hughes G, Pallini V, Hochstrasser DF and Tosi P: Protein expression profiles in human breast ductal carcinoma and histologically normal tissue. Electrophoresis *18*: 2832-2841, 1997.
40 Meyer-Siegler K and Hudson PB: Enhanced expression of macrophage migration inhibitory factor in prostatic adenocarcinoma metastases. Urology *48*: 448-452, 1996.
41 Kamimura A, Kamachi M, Nishihira J, Ogura S, Isobe H, Dosaka-Akita H, Ogata A, Shindoh M, Ohbuchi T and Kawakami Y: Intracellular distribution of macrophage migration inhibitory factor predicts the prognosis of patients with adenocarcinoma of the lung. Cancer *89*: 334-341, 2000.
42 Diffee GM, Kalfas K, Al-Majid S and McCarthy DO: Altered expression of skeletal muscle myosin isoforms in cancer cachexia. Am J Physiol Cell Physiol *283*: 1376-1382, 2002.
43 Acharyya S, Ladner KJ, Nelsen LL, Damrauer J, Reiser PJ, Swoap S and Guttridge DC: Cancer cachexia is regulated by selective targeting of skeletal muscle gene products. J Clin Invest *114*: 370-378, 2004.
44 Madhavan M and Krishnan KB: Cell marker studies in undifferentiated soft tissue sarcoma. Indian J Pathol Microbiol *34*: 99-103, 1991.
45 Schmidt D, Reimann O, Treuner J and Harms D: Cellular differentiation and prognosis in embryonal rhabdomyosarcoma. A report from the Cooperative Soft Tissue Sarcoma Study 1981 (CWS 81). Virchows Arch A Pathol Anat Histopathol *409*: 183-194, 1986.
46 Pawel BR, Hamoudi AB, Asmar L, Newton WA, Jr., Ruymann FB, Qualman SJ, Webber BL and Maurer HM: Undifferentiated sarcomas of children: pathology and clinical behavior–an Intergroup Rhabdomyosarcoma study. Med Pediatr Oncol *29*: 170-180, 1997.
47 Anagnostopoulos G, Sakorafas GH, Grigoriadis K and Kostopoulos P: Malignant fibrous histiocytoma of the liver: a case report and review of the literatures. Mt Sinai J Med *72*: 50-52, 2005.
48 Prasad S, Soldatenkov VA, Srinivasarao G and Dritschilo A: Intermediate filament proteins during carcinogenesis and apoptosis (Review). Int J Oncol *14*: 563-570, 1999.
49 Urbani A, Poland J, Bernardini S, Bellincampi L, Biroccio A, Schnolzer M, Sinha P and Federici G: A proteomic investigation into etoposide chemo-resistance of neuroblastoma cell lines. Proteomics 2005.
50 Byun Y, Chen F, Chang R, Trivedi M, Green KJ and Cryns VL: Caspase cleavage of vimentin disrupts intermediate filaments and promotes apoptosis. Cell Death Differ *8*: 443-450, 2001.
51 Woitge HW, Oberwittler H, Heichel S, Grauer A, Ziegler R and Seibel MJ: Short- and long-term effects of ibandronate treatment on bone turnover in Paget disease of bone. Clin Chem *46*: 684-690, 2000.

Received July 7, 2005
Revised September 16, 2005
Accepted September 19, 2005